



An extrusion–shear–expanding process for manufacturing AZ31 magnesium alloy tube

Ye TIAN¹, Hong-jun HU¹, Hui ZHAO¹, Wei ZHANG¹, Peng-cheng LIANG¹, Bin JIANG², Ding-fei ZHANG²

1. College of Materials Science and Engineering, Chongqing University of Technology, Chongqing 400050, China;
2. National Engineering Research Center for Magnesium Alloys, Chongqing University, Chongqing 400044, China

Received 17 June 2021; accepted 7 January 2022

Abstract: A new severe plastic deformation method for manufacturing tubes made of AZ31 magnesium alloy with a large diameter was developed, which is called the TCESE (tube continuous extrusion–shear–expanding) process. The process combines direct extrusion with a two-step shear–expanding process. The influences of expanding ratios, extrusion temperatures on the deformation of finite element meshes, strain evolution and flow velocity of tube blanks during the TCESE process were researched based on numerical simulations by using DEFORM-3D software. Simulation results show that the maximum expanding ratio is 3.0 in the TCESE process. The deformation of finite element meshes of tube blanks is inhomogeneous in the shear–expanding zone, and the equivalent strains increase significantly during the TCESE process of the AZ31 magnesium alloy. A extrusion temperature of 380 °C and expanding ratio of 2.0 were selected as the optimized process parameters from the numerical simulation results. The average grain size of tubes fabricated by the TCESE process is approximately 10 μm. The TCESE process can refine grains of magnesium alloy tubes with the occurrence of dynamic recrystallization. The (0001) basal texture intensities of the magnesium alloy tube blanks decrease due to continuous plastic deformation during the TCESE process. The average hardness of the extruded tubes is approximately HV 75, which is obviously improved.

Key words: AZ31 magnesium alloy; expanding ratio; continuous extrusion–shear; numerical simulation; microstructures

1 Introduction

In recent years, magnesium alloys have attracted considerable attention in industry and scientific fields due to their excellent properties, such as low density, high specific strength and good thermal conductivity [1–3]. Magnesium alloys are the preferred materials because they have lightweight, save energy and protect the environment and have been used in aerospace, automobile and other fields [4,5]. Unfortunately, the plasticity and fracture of magnesium alloy are of great challenge because of its hexagonal closed packed (HCP) crystal structure with few slip systems at room temperature and the deformation

mechanism of twinning and slip, which has not yet been well understood [6–8]. Critical shear stress is the precondition for the activation of slip systems. At room temperature, the critical shear stress required for basal plane slip is lower than that of prismatic and pyramidal slip. Under conventional conditions, prismatic and pyramidal slips do not easily activate [9,10]. Due to the poor plasticity of magnesium alloys at room temperature, the forming mode is generally hot processing compared with conventional metal processing [11,12]. Generally, applications of magnesium alloys have been limited by low formability.

One of the most common plastic processing methods for magnesium alloys is extrusion [13–16]. Extrusion is a process, in which the materials are

pushed or drawn through a die with expected cross-sections to create objects with a fixed cross-sectional profile. The extrusion process has been widely used in the production and forming of magnesium alloy tubes. For example, ABDOLVAND et al [17] combined parallel tube angular extrusion (PTCAP) and reverse extrusion to fabricate ultrafined AZ91 alloy thin-walled tubes, and the results showed that the ultimate strength, yield strength and microhardness of thin-walled tubes prepared by the composite process were remarkably improved. YU et al [18] used a novel severe plastic deformation method named rotary extrusion (RE) to manufacture cylindrical tubular parts with high-strength magnesium alloy. The results demonstrated that the microhardness of the tubes decreased with increasing rotary revolution, whereas the matrix and the second phases became significantly homogeneous. Dynamic recrystallization occurred during the RE process. SHEN et al [19] simulated the expanding extrusion of an AZ31 magnesium alloy tube by using DEFORM-3D software, and the optimal die angle was obtained.

In the present work, a new severe plastic deformation method for manufacturing tubes made of AZ31 magnesium alloy with a large diameter was developed. This process is called the TCESE (tube continuous extrusion–shear–expanding) process, which combines direct extrusion with a two-step shear–expanding process. The TCESE process contains the distinctive characteristics of severe plastic deformation. Moreover, there is great potential for the TCESE process to improve the mechanical properties and forming abilities of magnesium alloys, and magnesium alloy tubes with finer grains can be manufactured. The final grain sizes of the tubes are determined by process parameters such as extrusion temperatures of billets and dies, extrusion ratios, extrusion speeds, and friction coefficients.

The influences of expanding ratios and extrusion temperatures on the TCESE process were studied based on numerical simulations. The optimal expanding angles of the die were determined by simulations of DEFORM-3D software. Verification experiments of the TCESE process were carried out, and deformed microstructures and texture evolution for AZ31 magnesium alloy were studied.

2 Experimental

The experimental material was commercial AZ31 magnesium alloy. The dimensions of the AZ31 tube billets are as follows: the inner diameter is 17.5 mm, and the outer diameter is 39.8 mm. The extrusion temperature of the die and mandrel is 380 °C, and the extrusion speed is 5 mm/s. The experiments were conducted at an extrusion temperature of 380 °C. The parameters of the simulations and experiments are listed in Table 1. The experiments were carried out on a hydraulic equipment, as shown in Fig. 1(a). Heating bands, which are online heaters of dies, billets and thermocouples, are shown in Figs. 1(b) and (c), respectively. A thin-walled tube prepared by the TCESE process is indicated in Fig. 1(d). Figure 2 shows a finite element model of the TCESE process and an enlarged view of the forming part in the TCESE die. The forming part consists of four parts: an upsetting zone, a first shear–expanding zone, a second shear–expanding zone and a sizing zone. Tubes with large diameters that are approximately 2 times those of the original tubes can be prepared by the TCESE process.

The specimens of the upsetting zone, first shear–expanding zone, second shear–expanding zone and sizing zone prepared by the TCESE process were observed by optical microscopy (OM).

Table 1 Parameters of simulations and experiments for TCESE process

Parameter	Value
Inner diameter of tube blank/mm	17.5
Outer diameter of tube blank/mm	39.8
Length of tube blank/mm	80
Expanding ratio of tube	1.3, 1.6, 2.0, 2.5, 3.0
Expanding angle/(°)	140
Extrusion temperature of tube blank/°C	380
Extrusion speed/(mm·s ⁻¹)	5
Number of mesh	32000
Coefficient of thermal conductivity between die and blank/(N·°C ⁻¹ ·s ⁻¹ ·mm ⁻²)	11
Simulation step size/mm	0.2
Mesh density type	Relative
Friction factor between billet and die	0.3

The microstructures and textures of the four zones were analyzed by electron backscatter diffraction (EBSD).

The direction of sample selection is along the extrusion direction (ED). The sampling locations of

the four parts for hardness testing and EBSD testing are shown in Fig. 3(a). Lateral sampling positions in each zone are shown in Fig. 3(b). As shown in Fig. 3(c), the specimens are machined into rectangular samples.

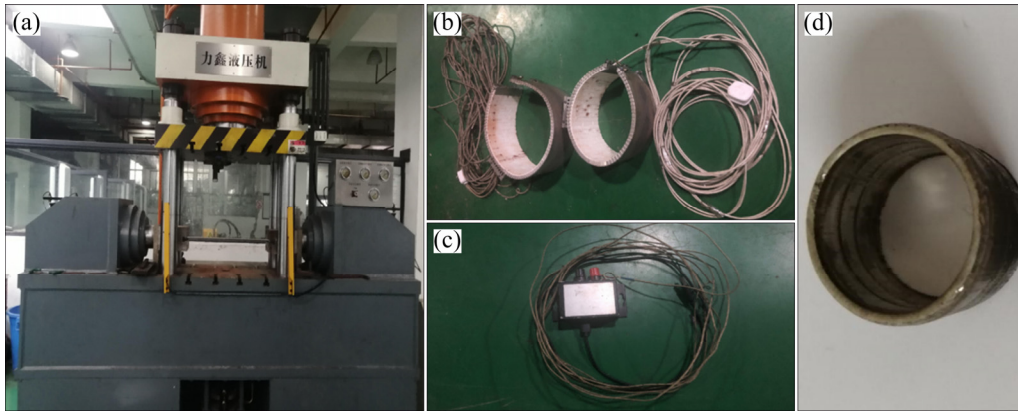


Fig. 1 Experimental equipment and formed tube prepared by TCESE process: (a) Hydraulic equipment; (b) Heating coils; (c) Thermocouple; (d) Tube prepared by TCESE process

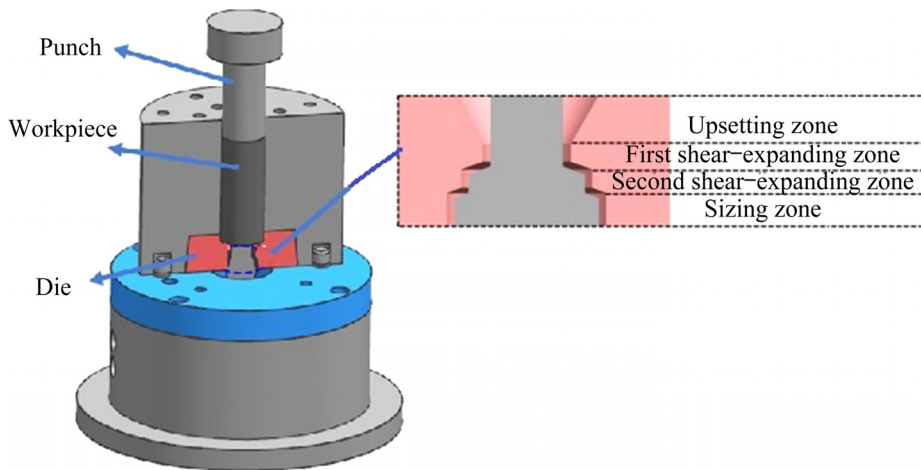


Fig. 2 Finite element model of TCESE process and enlarged view of forming part in TCESE die

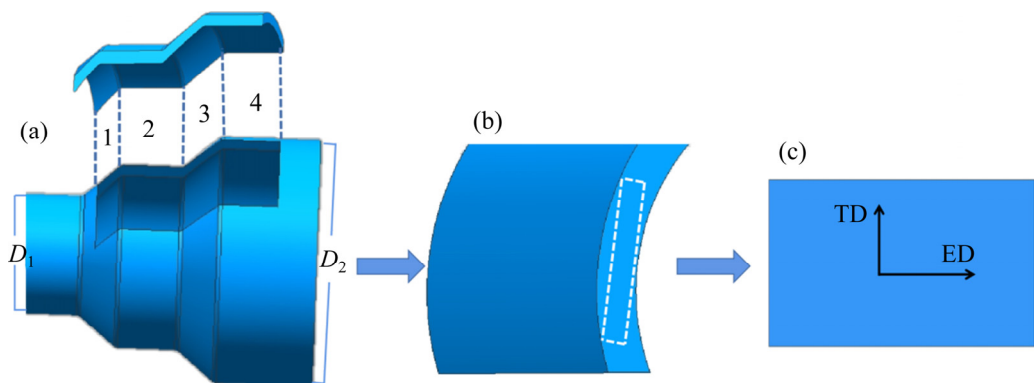


Fig. 3 Sampling locations of hardness and EBSD testing: (a) Sampling along extrusion direction (1—Upsetting zone; 2—First shearing-expanding zone; 3—Second shear-expanding zone; 4—Sizing zone); (b) Lateral sampling position in each zone; (c) Rectangular specimen

3 Results and discussion

3.1 Influence of expanding ratio on deformation of finite element meshes

The selection of expanding ratio is very important to obtain magnesium alloy tubes with large diameter and high performance. The expanding ratio is defined as the ratio of the inner diameter for the sizing zone (D_2) to the inner diameter for the upsetting zone (D_1), as shown in Fig. 3(a). Figure 4 shows the deformation of finite element meshes in tube blanks with different expanding ratios (1.3, 1.6, 2.0, 2.5 and 3.0) during the TCESE process. From Fig. 4 it is found that the deformation of the finite element meshes in the tube blanks is uniform in the upsetting zone. However, with increasing expanding ratio, the deformation of finite element meshes is uneven in the shear-expanding zone. The plastic deformation of tube blanks becomes more difficult if the expanding ratio is larger because the resistance of plastic deformation increases and the fluidity of metal decreases. As shown in Figs. 4(a) and (b), the meshes in the tube blank are uniform after plastic deformation when the expanding ratio is less than 2.0, which implies that the quality of the tube is good. When the diameter expanding ratio is 2.5, the uniformity of the deformation meshes worsens. If the expanding ratio reaches 3.0, the deformation meshes of the tube blank become very asymmetric, and the wall of the formed tube is uneven. With

increasing expanding ratio, the fluidity of the blank is different. Parts of the tube walls are preferentially formed during the TCESE process, and the metal flow is insufficient because the formed tube walls are asymmetric, which leads to the formation of defects in the tubes [20].

3.2 Strain evolution during TCESE processes with different expanding ratios

The deformation zone can be divided into four parts mainly during the process of deformation, which include the upsetting zone, first shear-expanding zone, second shear-expanding zone, and sizing zone. Figure 5 shows the distribution of equivalent strains with different expanding ratios, which shows that the equivalent strains of the tubes increase with increasing expanding ratios. The plastic deformation of TCESE processes becomes intenser with increasing expanding ratio. The strain of the second shear-expanding zone is the largest during the TCESE process. When the expanding ratio is 1.6, the strain in the deformation zone of the blank is small, and the strain distribution is uniform. The average value of strains is approximately 5 in the blank of the shear-expanding zone. With increasing expanding ratios, the discrepancy in deformation also increases, and the strains of the blanks in the shear-expanding zone obviously increase. When the expanding ratio is 3.0, the strain value of the blank in the shear-expanding zone is approximately 12, and the equivalent strain is approximately 10. Rising the

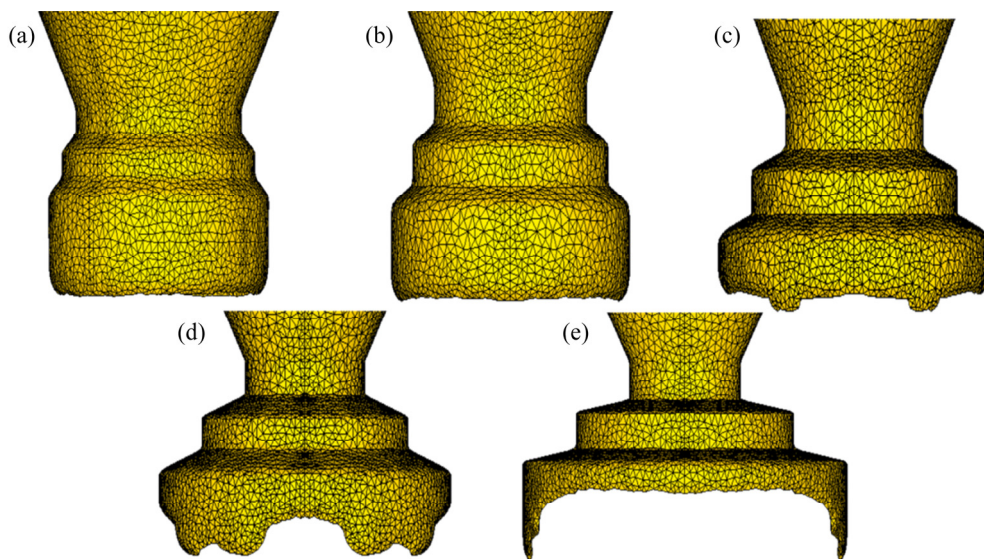


Fig. 4 Deformation of finite element meshes in tube blanks during TCESE processes with different expanding ratios: (a) 1.3; (b) 1.6; (c) 2.0; (d) 2.5; (e) 3.0

expanding ratio will reduce the strain uniformity in the deformation zone. The expanding ratio could affect the uniformity of strains during the deformation process. If the expanding ratio is too large, compressive stresses will exert allowable limit values on the tube blanks during the TCSE process.

3.3 Flow velocities for tube blanks during TCSE process

The analysis of flow velocity fields was carried out by point tracking. Three designated points (P_1 , P_2 and P_3) were selected as shown in Fig. 6. P_1 is the point on the inner wall of the tube blank, and P_2 and P_3 are points on the outer wall of the tube blank. It can be seen from Fig. 6 that the flow velocities of the alloy near the outer walls of the tube blanks are faster than those near the inner wall during the early stage of the TCSE process. However, the flow velocities near the inner wall are faster than those near the outer wall in the

shear-expanding zone. The flow velocity differences between the inner and outer parts of the tube blanks are beneficial to the formation of shear stress, which is favorable for the dynamic recrystallization [21].

3.4 Textures of magnesium alloy tubes in different zones

Thin-walled tubes were prepared successfully by the TCSE process with a extrusion temperature of 380 °C and an expanding ratio of 2.0. Pole figures and inverse pole figures (IPF) of the magnesium alloy tubes in different zones are shown in Fig. 7. The textures of magnesium alloy tubes in four zones were analyzed.

The pole figure and inverse pole figure for the (0001) basal plane in the upsetting zone during the TCSE process are shown in Fig. 7(a). The pole figure shows that the basal plane of grains is parallel to the extrusion direction, and the texture type is typical of the basal texture of extruded

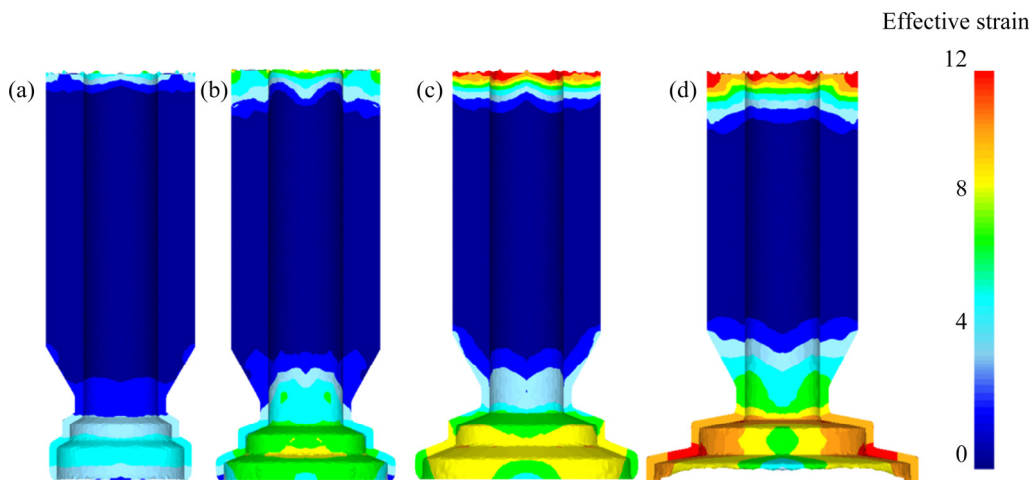


Fig. 5 Strain distribution during TCSE process with different expanding ratios: (a) 1.6; (b) 2.0; (c) 2.5; (d) 3.0

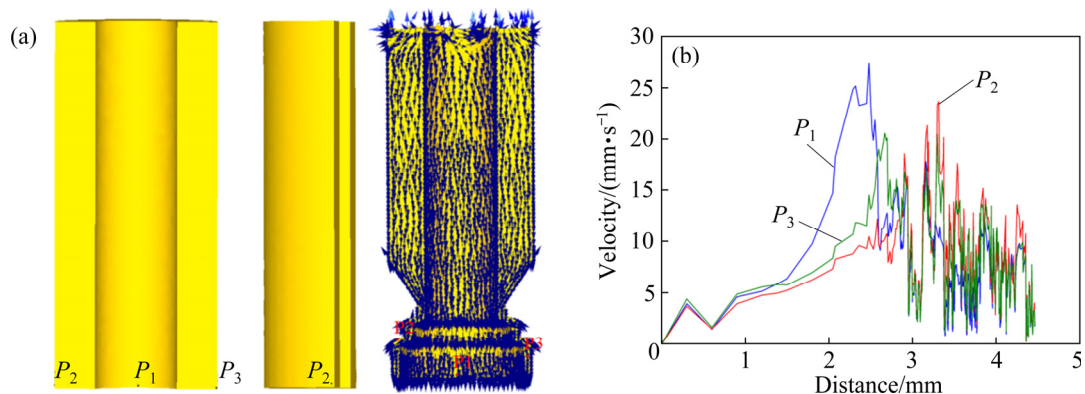


Fig. 6 Velocity distribution of tube blanks during TCSE process with expanding ratio of 2.0: (a) Tube blank and three designated point positions; (b) Point tracking of three points

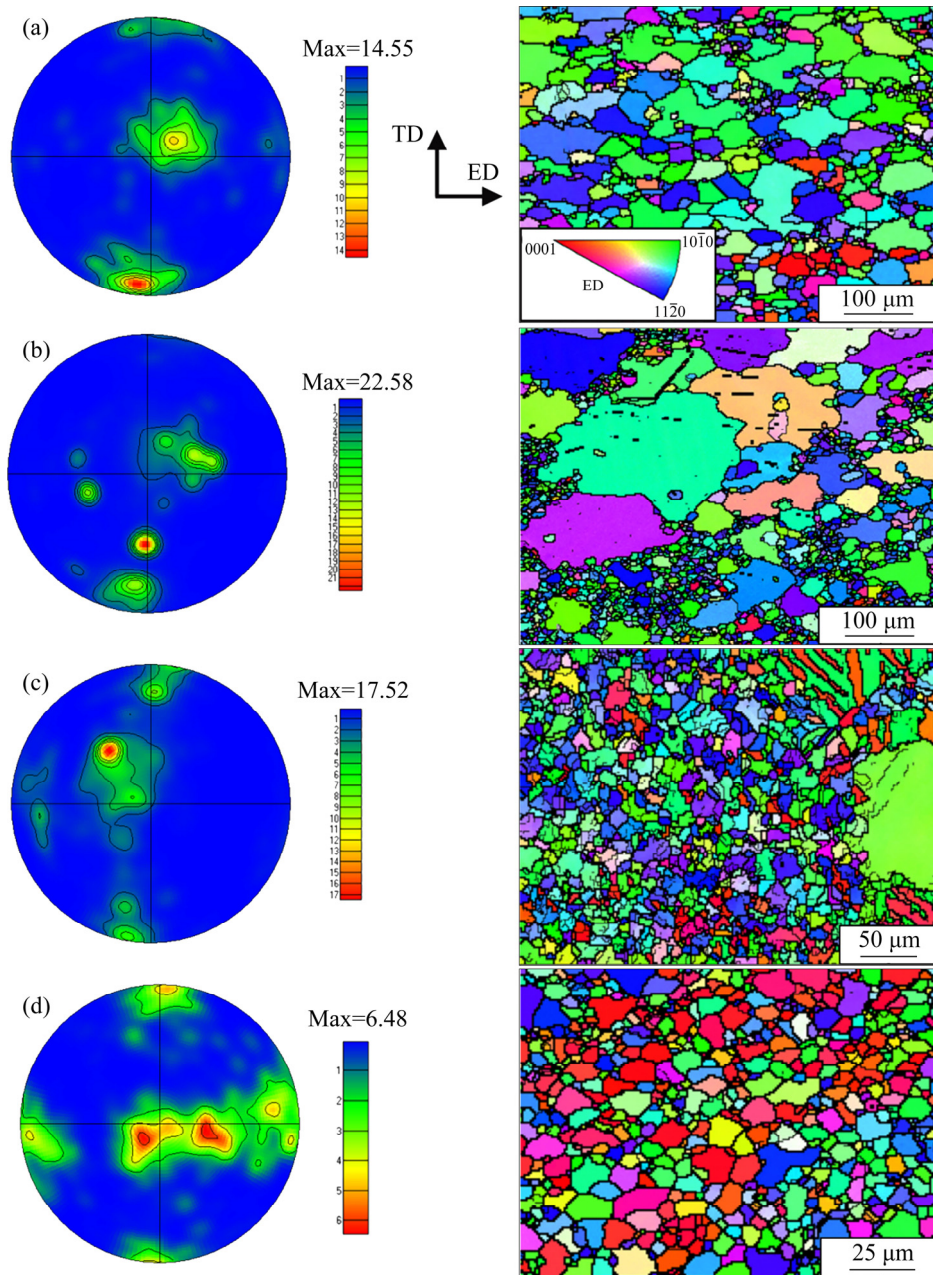


Fig. 7 Pole figures and inverse pole figures for (0001) basal plane in different deformation zones during TCSE process: (a) Upsetting zone; (b) First shear-expanding zone; (c) Second shear-expanding zone; (d) Sizing zone

magnesium alloy. The grains are subjected to strong compressive stresses from three directions in the upsetting zone.

In the first shear-expanding zone, the tube blanks are subjected to shearing forces; however, the downward compressive stress is still dominant. Therefore, as shown in Fig. 7(b), the texture intensities increase, and the orientations of some grains change accordingly. The dispersion degree of polar coordinates varies little. Dynamic recrystallization of magnesium alloy will occur if accumulative strains and shear forces exerted

by the TCSE process reach certain critical values [22–24]. Large numbers of fined dynamic recrystallized grains are distributed among the grain boundaries. When the tube blank flows through the second shear-expanding zone, the grain orientations change greatly. The basal textures are distributed along the ED, as shown in Fig. 7(c). The grain orientation deflects along the ED. The texture strengths are reduced compared with those in the first shear-expanding zone. The overall pole figures are more diffusive.

Figure 7(d) shows the pole figure and inverse

pole figure in the sizing zone. The (0001) basal plane of most grains obviously deflects. But, there is still basal texture along the ED, and the texture strengths are obviously weakened. The pole figure becomes more scattered compared with that of Fig. 7(c).

On the one hand, magnesium alloy tubes have undergone two shear deformations during the TCESE process. The grain orientations of magnesium alloy fabricated by the TCESE process tilt toward the principal stress axis. On the other hand, the second shear-expanding deformations will increase the accumulative strains. Dynamic recrystallization of magnesium alloy occurs during continuous shears of the TCESE process [25,26]. The dynamic recrystallization degree was affected, and the grain orientation changed accordingly. In general, the preferred orientations of the basal plane in most grains distributed along the ED direction might be weakened by the TCESE process, and the orientations of grains become random.

It can be seen from Fig. 7 that the microstructures of the tube blanks change significantly. The grains change obviously in different zones due to the occurrence of dynamic recrystallization. In the first shear-expanding zone, recrystallized grains appear. Uniform equiaxed grains appear in the sizing zone because the grains are refined significantly by repeated continuous shear-expanding deformation. The average grain size of the thin-walled tube fabricated by the TCESE process is approximately 10 μm .

3.5 Hardness distribution

The results of hardness testing for the thin-walled tubes prepared by the TCESE process are depicted in Fig. 8. The hardness values were measured in the upsetting zone, the first shear-expanding zone, the second shear-expanding zone, and the sizing region. The average hardness of magnesium alloy in the upsetting zone is approximately HV 57, and the values of magnesium alloy in the first and second shear-expanding zones increase to HV 67 and HV 78, respectively. The average hardness of the sizing zone is approximately HV 75. The hardness is obviously improved by the TCESE process. The grain refinement of magnesium alloy in thin-walled tubes prepared by the TCESE process is considered one main reason for the hardness increase [27,28].

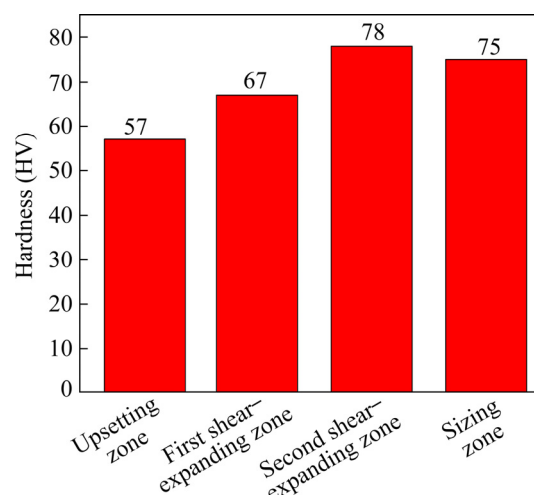


Fig. 8 Hardness of different zones of tube blank fabricated by TCESE process (error range: \pm HV 1)

4 Conclusions

(1) Thin-walled tubes were successfully prepared by the TCESE process at an extrusion temperature of 380 $^{\circ}\text{C}$ and an expanding ratio of 2.0, and their diameters were approximately 2 times those of the original tubes.

(2) The influences of expanding ratios on the deformation of finite element meshes and strain evolution show that the maximum expanding ratio is 3.0 for the TCESE process. The flow velocities of the alloy near the outer and inner walls of the tube blanks are different during the TCESE process.

(3) Texture analysis results show that the TCESE process can refine grains of magnesium alloy tubes with the occurrence of dynamic recrystallization. The average grain size of tubes fabricated by the TCESE process is approximately 10 μm . The basal plane of grains is parallel to the ED in the upsetting zone. The texture intensities increase, and the orientations of some grains change accordingly in the first shear-expanding zone. The grain orientation of the second shear-expanding zone deflects along the ED, and the texture strengths are reduced. The preferred orientations of the basal plane in most grains distributed along the ED in the sizing zone might be weakened by the TCESE process, and the orientations of grains become random. The decrease of the (0001) basal texture intensities for magnesium alloy tube blanks is due to continuous plastic deformation.

(4) The hardness of the AZ31 magnesium alloy was obviously improved by the TCESE process for

grain refinement of the magnesium alloy during the TCESE process.

Acknowledgments

This work was financially supported by the National Natural Science Foundation of China (Nos. 52071042, 51771038), the Chongqing Talent Plan, China (No. CQYC202003047), and Chongqing Natural Science Foundation, China (Nos. cstc2018jcyjAX0249, cstc2018jcyjAX0653).

References

- [1] SHI Bao-liang, LUO Tian-jiao, WANG Jing, YANG Yuan-sheng. Hot compression behavior and deformation microstructure of Mg–6Zn–1Al–0.3Mn magnesium alloy [J]. Transactions of Nonferrous Metals Society of China, 2013, 23(9): 2560–2567.
- [2] WANG Li-fei, HUANG Guang-sheng, LI Hong-cheng, ZHANG Hua. Influence of strain rate on microstructure and formability of AZ31B magnesium alloy sheets [J]. Transactions of Nonferrous Metals Society of China, 2013, 23(4): 916–922.
- [3] DAVOODI F, ATAPOUR M, BLAWERT C, ZHELUDKEVICH M. Wear and corrosion behavior of clay containing coating on AM 50 magnesium alloy produced by aluminate-based plasma electrolytic oxidation [J]. Transactions of Nonferrous Metals Society of China, 2021, 31(12): 3719–3738.
- [4] YANG Yan, XIONG Xiao-ming, CHEN Jing, PENG Xiao-dong, CHEN Dao-lun, PAN Fu-sheng. Research advances in magnesium and magnesium alloys worldwide in 2020 [J]. Journal of Magnesium and Alloys, 2021, 9(3): 705–747.
- [5] AHMADI S, ALIMIRZALOO V, FARAJI G, DONIAVI A. Properties inhomogeneity of AM60 magnesium alloy processed by cyclic extrusion compression angular pressing followed by extrusion [J]. Transactions of Nonferrous Metals Society of China, 2021, 31(3): 655–665.
- [6] DING Wen-jiang, JIN Li, WU Wen-xiang, DONG Jie. Texture and texture optimization of wrought Mg alloy [J]. The Chinese Journal of Nonferrous Metals, 2011, 21(10): 2371–2381. (in Chinese)
- [7] LAN Yong-ting, CHEN Yuan, REN Yi-fang, ZHANG Ke-shi, WANG Shuai. Constitutive model based on slip and twinning of AZ31 Mg alloy and analysis of microstructural relatedness [J]. The Chinese Journal of Nonferrous Metals, 2019, 29(8): 1660–1675. (in Chinese)
- [8] LAN Yong-ting, ZHONG Xian-ci, QUAN Gao-feng, LING Ruo-cheng, ZHANG Ke-shi. Crystal anisotropy of AZ31 magnesium alloy under uniaxial tension and compression [J]. Transactions of Nonferrous Metals Society of China, 2015, 25(1): 249–260.
- [9] SONG Bo, XIN Ren-long, GUO Ning, LIU Ting-ting, YANG Qing-shan. Research progress of strain hardening behavior at room temperature in wrought magnesium alloys [J]. The Chinese Journal of Nonferrous Metals, 2014, 24(11): 2699–2710. (in Chinese)
- [10] LIU Ting-ting, PAN Fu-sheng. Development and application of “solid solution strengthening and ductilizing” for magnesium alloys [J]. The Chinese Journal of Nonferrous Metals, 2019, 29(9): 2050–2063. (in Chinese)
- [11] WANG Bo-ning, WANG Feng, WANG Zhi, LIU Zheng, MAO Ping-li. Fabrication of fine-grained, high strength and toughness Mg alloy by extrusion-shearing process [J]. Transactions of Nonferrous Metals Society of China, 2021, 31(3): 666–678.
- [12] WANG Jing-feng, PENG Xing, WANG Kui, WANG Qing, GAO Shi-qing. Numerical simulation and experimental study on extrusion forming of ultralarge size wide thin-walled hollow magnesium alloy profiles [J]. The Chinese Journal of Nonferrous Metals, 2020, 30(12): 2809–2819. (in Chinese)
- [13] SHI Lei, MIN Zhi-Yu, HE Jun-Guang, YAO huai, LIU Ya. Optimization of process parameters for ZK60 magnesium alloy hollow plate in P-ECAP extrusion [J]. The Chinese Journal of Nonferrous Metals, 2019, 29(6): 1161–1169. (in Chinese)
- [14] LE Tai-he, CHEN Meng-ru, WANG Jin-hui, JIN Pei-peng. Effect of La and Ce contents on microstructure, texture and mechanical properties of extruded AE44-2 magnesium alloy [J]. The Chinese Journal of Nonferrous Metals, 2021, 31(6): 1463–1474. (in Chinese)
- [15] LIU Jun-wei, CHEN Zhen-hua, CHEN Ding, LI Gui-fa. Deformation mechanism and softening effect of extruded AZ31 magnesium alloy sheet at moderate temperatures [J]. Transactions of Nonferrous Metals Society of China, 2012, 22(6): 1329–1335.
- [16] HU Ju-zong, LIU Yan-feng, LU Li-wei, WU Xian-peng, LIU Chu-ming. Continuous deformation technology and extrusion load calculation of Mg alloy fabricated by direct extrusion and bending shear deformation [J]. Transactions of Nonferrous Metals Society of China, 2018, 28(5): 923–930.
- [17] ABDOLVAND H, FARAJI G, SHAHBAZI K J. Microstructure and mechanical properties of fine-grained thin-walled AZ91 tubes processed by a novel combined SPD process [J]. Bulletin of Materials Science, 2017, 40(7): 1471–1479.
- [18] YU Jian-min, ZHANG Zhi-min, WANG Qiang, HAO Hong-yuan. Rotary extrusion as a novel severe plastic deformation method for cylindrical tubes [J]. Materials Letters, 2018, 215: 195–199.
- [19] SHEN Qun, WU Zhi-lin, YUAN Ren-shu, SONG De-feng. Numerical simulation of tube-expanding extrusion process of magnesium alloy [J]. Hot Working Technology, 2013, 42(7): 82–85. (in Chinese)
- [20] HU Bo, LI Dejiang, LI Zi-xi, ZENG Xiao-qin, DING Wen-jiang. Research progress on hot tearing behavior of cast magnesium alloys [J]. Journal of Net-shape Forming Engineering, 2020, 12(5): 1–19.
- [21] FENG Jin-kai, ZHANG Ding-fei, YUAN Yuan, CHEN Xia, ZHAO Yang, JIANG Bing, PAN Fu-sheng. Effect of extrusion-shear angle on microstructure and properties of AZ31 magnesium alloy [J]. Transactions of Materials and Heat Treatment, 2019, 40(12): 159–168.

- [22] DU P H, FURUSAWA S, FURUSHIMA T. Continuous observation of twinning and dynamic recrystallization in ZM21 magnesium alloy tubes during locally heated dieless drawing [J]. *Journal of Magnesium and Alloys*, 2022, 10(3): 730–742.
- [23] HU Yan, HU Lian-xi, SUN Yu. Dynamic recrystallization kinetics of as-cast AZ91D alloy [J]. *Transactions of Nonferrous Metals Society of China*, 2014, 24(6): 1683–1689.
- [24] LI Xin, JIANG Jing-hua, ZHAO Yong-hao, MA Ai-bin, WEN Dao-jing, ZHU Yun-tian. Effect of equal-channel angular pressing and aging on corrosion behavior of ZK60 Mg alloy [J]. *Transactions of Nonferrous Metals Society of China*, 2015, 25(12): 3909–3920.
- [25] AYER Ö. A forming load analysis for extrusion process of AZ31 magnesium [J]. *Transactions of Nonferrous Metals Society of China*, 2019, 29(4): 741–753.
- [26] SIAHSARANI A, FARAJI G. Processing and characterization of AZ91 magnesium alloys via a novel severe plastic deformation method: Hydrostatic cyclic extrusion compression (HCEC) [J]. *Transactions of Nonferrous Metals Society of China*, 2021, 31(5): 1303–1321.
- [27] XIA Yu, WU Liang, YAO Wen-hui, HAO Meng, CHEN Jing, ZHANG Cheng, PAN Fu-sheng. In-situ layered double hydroxides on Mg–Ca alloy: Role of calcium in magnesium alloy [J]. *Transactions of Nonferrous Metals Society of China*, 2021, 31(6): 1612–1627.
- [28] DING Yun-long, WANG Jian-gang, ZHAO Ming, JU Dong-ying. Effect of annealing temperature on joints of diffusion bonded Mg/Al alloys [J]. *Transactions of Nonferrous Metals Society of China*, 2018, 28(2): 251–258.

一种 AZ31 镁合金管材挤压–剪切–扩径成形工艺

田野¹, 胡红军¹, 赵辉¹, 张威¹, 梁鹏程¹, 蒋斌², 张丁非²

1. 重庆理工大学 材料科学与工程学院, 重庆 400050;

2. 重庆大学 国家镁合金材料工程技术研究中心, 重庆 400044

摘要: 设计一种新型大塑性变形方法(管材连续挤压–剪切–扩径(TCESE)工艺)制备 AZ31 镁合金扩径管材。采用直接挤压与两道次剪切–扩径相结合的工艺, 利用 DEFORM-3D 有限元软件, 研究 TCESE 工艺中扩径比与挤压温度对坯料有限元网格变化、应变分布和流动速度的影响。模拟结果表明, 在 TCESE 过程中, 管材最大的扩径比可达 3.0, 坯料网格变化在剪切–扩径区是不均匀的, 在扩径成形阶段等效应变显著增大。根据有限元模拟结果, 选择 380 °C 的挤压温度和 2.0 的扩径比为最优工艺参数, 在该参数下制备的管材平均晶粒尺寸约为 10 μm, 动态再结晶的发生为扩径挤压晶粒细化的主要原因。扩径管材(0001)基面织构强度在 TCESE 工艺中由于连续的塑性变形而降低。TCESE 工艺制备的扩径管材的平均硬度明显增大, 约为 HV 75。

关键词: AZ31 镁合金; 扩径比; 连续挤压–剪切; 数值模拟; 显微组织

(Edited by Wei-ping CHEN)